



The “vermian–crest angle”: does it allow accurate categorisation of fetal upward rotation of cerebellar vermis on intrauterine MRI? A pilot study

M. Spinelli^{a,*}, R. Wiest^b, L. Di Meglio^c, M. Baumann^d, L. Raio^d,
D. Surbek^d

^a Department of Clinical Research, University of Bern, Bern, Switzerland

^b Department of Diagnostic and Interventional Neuroradiology, University of Bern, Bern, Switzerland

^c Private Centre “Diagnostica ecografica Aniello Di Meglio srl”, Naples, Italy

^d Department of Obstetrics and Gynecology, University of Bern, Bern, Switzerland

ARTICLE INFORMATION

Article history:

Received 6 November 2017

Accepted 21 February 2019

AIM: To test a new parameter to assess the position of the fetal cerebellar vermis in the posterior fossa (PF) using intrauterine magnetic resonance imaging (MRI).

MATERIALS AND METHODS: The angle between the cerebellar vermis and the internal occipital crest (vermian–crest angle, VCA) was assessed retrospectively using MRI in fetuses with and without PF anomalies. Spearman’s rank test was used to investigate correlation of the VCA with gestational age (GA). Groups were compared using Student’s *t*-test and the one-way analysis of variance (ANOVA) with the Bonferroni adjustment. Box-and-whisker plots were also used.

RESULTS: One hundred and two normal cases were identified. Mean±SD GA at MRI was 26.5±2.8 weeks (range: 22–32 weeks). The VCA was 64.49±11.5° independently of GA ($r=0.19$; $p=0.12$). In addition, 30 fetuses at 19–28 weeks were identified with Blake’s pouch cyst (BPC; $n=5$), Dandy–Walker malformation (DWM; $n=12$), mega cisterna magna (MCM; $n=10$), and vermian hypoplasia (VH; $n=3$). The VCA was significantly different in the DWM ($p<0.001$) and BPC ($p<0.001$) subgroups, but was not significantly different in cases of VH ($p=0.84$) and MCM ($p=0.95$) in comparison with controls.

CONCLUSIONS: A new method to assess vermian position within the PF using intrauterine MRI was assessed. In combination with the other existing parameters, it may be helpful for addressing the categorisation of upward rotation of the fetal cerebellar vermis; however, further studies are necessary to strengthen the present findings.

© 2019 The Royal College of Radiologists. Published by Elsevier Ltd. All rights reserved.

Introduction

The complementary role of intrauterine magnetic resonance imaging (MRI) in evaluating the abnormalities suspected at prenatal ultrasound (US) with higher spatial

* Guarantor and correspondent: M. Spinelli, Department of Clinical Research, University of Bern, Bern, Switzerland. Tel.: +41762773513.

E-mail address: marialuigiaspinelli@live.it (M. Spinelli).

resolution and tissue contrast has been increasingly recognised, and concerns about an abnormal posterior fossa (PF) is one of the main referral reasons for clinical MRI examination.^{1–3} Recently, some authors proposed “that any fetus with a suspected brain abnormality on ultrasound should have intrauterine MRI to better inform counselling and management decisions”.³

Indeed, in the case of an abnormal PF, differential diagnosis is challenging, ranging from benign asymptomatic conditions to severe malformations associated with neurological impairment.^{4–8} As an example, the four most common anomalies, Dandy–Walker malformation (DWM), vermian hypoplasia (VH), Blake’s pouch cyst (BPC), and mega cisterna magna (MCM), show similar sonographic characteristics but are associated with very different prognoses.⁹

A wide communication between the fourth ventricle and the PF, with a reduced size of the vermis, are the main features of most PF abnormalities; however, in accordance with a recent classification,¹⁰ the upward rotation of the vermis has been suggested as a key finding in the differential diagnosis. Unfortunately, both US and MRI evaluation of this critical finding are usually subjective, and no reference charts for normal and abnormal cases have been provided to date. Although there has been recent attention paid to vermian biometry, as well as some attempts to measure the angle between the vermis and PF structures (i.e., at the level of the pons and the tegmentum^{11–23}), an accurate categorisation of fetal upward rotation/hypoplasia of the vermis remains a challenge.

The aims of the present study were fourfold: (1) to test a new method to assess the normal position of the cerebellar vermis over the brainstem using a novel measurement, the angle between the cerebellar vermis and the internal occipital crest (vermian–crest angle, VCA) using intrauterine MRI; (2) to evaluate the reproducibility of these measurements between different operators; (3) to compare the MRI measurements with those obtained at three-dimensional (3D) US; and (4) to compare these measurements with those obtained at MRI in cases with an abnormal PF.

Materials and methods

A retrospective study of all intrauterine MRI examinations performed between January 2008 and January 2017 at the Department of Diagnostic and Interventional Neuroradiology was conducted by searching the fetal imaging databases. The present study was undertaken in accordance with the Declaration of Helsinki and was approved by the Review Board of the Department of Clinical Research, University of Bern. All adult participants provided written informed consent to participate in the study. The cases included patients from a screening population referred to the Department of Obstetrics and Gynecology, comprising approximately 7,500 pregnant women examined per year. MRI examinations were performed due to increased risk of suspected cerebral pathology, including suspected infectious fetopathy, assumed cerebral abnormality at US,

positive family history for cerebral abnormalities, decreased fetal movements, idiopathic polyhydramnios, as well as in cases with extracranial anomalies. Only those cases in which the suspicion of cerebral anomalies was not confirmed at MRI and in which there was no evidence of intracranial abnormalities at birth were included in the control group. The other inclusion criteria for the controls were the following: singleton pregnancy, good dating, normal obstetric course (no evidence of intrauterine growth restriction, macrosomia, or pregnancy-related hypertensive disorders), absence of maternal medical diseases, neonatal birth weight within the 10th to the 90th percentiles, and clinically normal fetus at birth (normal Apgar [Appearance, Pulse, Grimace, Activity, Respiration] scores, normal neonatal physical examination findings).

Inclusion criteria for pathology groups were availability of detailed postnatal data as well as availability of MRI digital images of good quality. The quality of the MRI images was assessed by the reviewing radiologist (R.W.). Visual quality assessment was done by scoring the visibility of the structures within the PF using a five-point scale. A score of 1 reflected excellent visualisation, whereas a score of 5 reflected non-diagnostic images. Only the pictures classified with a score 1 or 2 were used for the study.

In pathological cases, the following clinical data were recorded: gestational age (GA), fetal sex, associated anomalies, maternal age, singleton or multiple gestation, fetal karyotype (if available), GA at birth, mode of delivery, postnatal neonatal examination including neurosonography, and, in the case of intrauterine or neonatal death or pregnancy termination, pathology reports.

Intrauterine MRI examinations were performed using a Siemens Magnetom Sonata or Avanto 1.5 T system (Siemens Medical Systems, Erlangen, Germany) using a four-channel body phased-array coil combined with channels from the spine array coil adjacent to the fetus. Depending on patient comfort, patients were positioned supine or on the left lateral side. Intravenous contrast medium or sedative premedication were not used. The standard protocol included T1-weighted fast-low angle shot (FLASH; repetition time [TR] = 85 ms, echo time [TE] = 4.76 ms, flip angle = 70°), T2-weighted half-Fourier acquired single-shot turbo-spin echo (HASTE; TR = 1,260 ms, TE = 84 ms), T1-weighted inversion recovery (TR = 9,470 ms, TE = 17 ms), and T2-weighted true fast imaging with steady procession (FISP; TR = 4.3 ms, TE = 1.86 ms; all three gradients refocused) sequences with a section thickness of 3 mm and one acquisition. For all sequences, the field of view (320–400 mm) and acquisition matrix (256–448 mm) were adapted to the size of the mother to gain an in-plane resolution of 1.25×1.25 mm or less. In all patients, axial and coronal images were acquired by HASTE sequences, which were evaluated for the purposes of this study. The number of sections varied according to section orientation and size of the fetus. The mean imaging duration was approximately 40 minutes.

For the study of the PF, contiguous orthogonal sections in the axial, coronal, and sagittal plane with a section thickness of 3 mm were included. Two landmarks were used for the measurements: (1) the nodulus vermis, at the level of

the fastigial peak of the fourth ventricle, as described in the literature,⁹ and (2) the internal occipital crest, visible posterior to the cerebellar vermis at the level of the attachment on the falx cerebella, as previously reported.²³ Based on these landmarks, the VCA was measured, defined by the convergence of two lines: the first, tangent to the internal occipital crest; the second, tangent to the nodulus vermis (Fig 1). All measurements were performed by a single operator.

To evaluate the reproducibility of the measurements, an arbitrary sample of 18 fetuses was evaluated twice by the first operator and then by a second operator. Each operator was unaware of the results obtained by the other. In these cases, the two operators were identified as no. 1 (senior, i.e., >5 years of experience in MRI prenatal diagnosis) and no. 2 (junior, i.e., <5 years of experience in MRI prenatal diagnosis), and all measurements were numbered as 1 or 2 when performed by the senior and the junior operator, respectively, as previously reported.¹¹

All MRI measurements in normal cases were compared with those obtained at prenatal three-dimensional (3D) US, using the same plane and landmarks described for MRI and the technique already reported^{23–25} in a cross-sectional, prospective cohort of 81 physiological pregnancies within the same GA range. The measurements in normal cases (control group) were compared with those obtained at MRI in cases with PF abnormalities (pathology groups).

Statistical analysis was performed using Graph-Pad Prism version 5.00 for Windows, (Graph-Pad Software, San Diego CA) and SPSS statistical software (version 19.0; SPSS Inc., Chicago, IL, USA). Correlations of the VCA with GA were searched using Spearman's rank test. A comparison among groups was performed using Student's *t*-test and one-way analysis of variance with the Bonferroni adjustment, after checking the normality of the distribution (one sample Kolmogorov–Smirnov test). Box-and-whisker plots were also used. Interobserver variability for the VCA was

assessed by interclass correlation coefficients (ICCs). Values <0.5, between 0.5 and 0.75, between 0.75 and 0.9, and >0.90 were considered indicative of poor, moderate, good, and excellent reliability, respectively.²⁶ Statistical significance was considered achieved when $p < 0.05$.

Results

One hundred and two cases with normal brain anatomy were selected from the prenatal imaging database and were suitable for analysis. Adequate measurement of the VCA was obtained in all cases. Mean±SD of GA at inclusion was 26.5±2.8 weeks (range: 22–32). Mean±SD of VCA was 64.49±11.5 within the investigated gestation age period. No correlation was found between VCA and GA ($r=0.19$; $p=0.12$). When MRI measurements were compared with those performed at 3D US, Student's *t*-test showed that MRI and US measurements did not differ significantly ($p=0.11$). When the interobserver variability for VCA was assessed in the series of 18 fetuses, the ICC was 0.85 (95% CI: 0.656–0.933).

During the study period, complete records from 30 fetuses fulfilling the inclusion criteria were available with PF abnormalities (five with BPC, 12 with DWM, three with VH, 10 with MCM). Table 1 shows the clinical characteristics of the pathology group, including perinatal outcome data.

The VCA was significantly changed in the DWM (150.57±15.78; $p \leq 0.001$) and BPC (100.25±6.05; $p \leq 0.001$) subgroups of anomalies (Fig 2); the angle increased progressively with the severity of the condition according to a continuum: a VCA of <85° was within the normal range, a measurement of >85° was found in cases of BPC, while a VCA of >107° was suggestive of a DWM (Table 2). On the

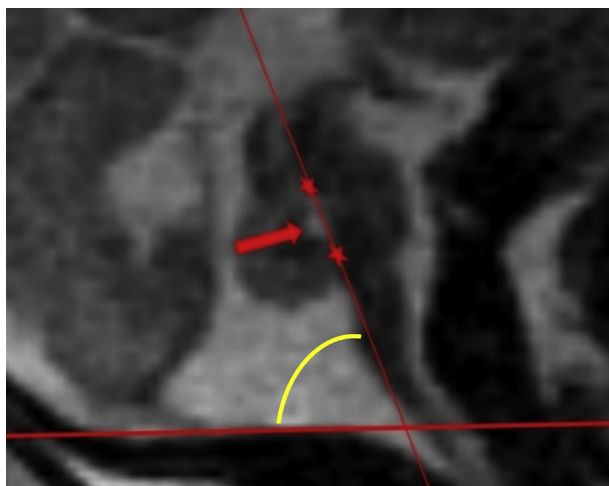


Figure 1 MRI midsagittal view of the PF in a 25-week-old fetus. The VCA is labelled in yellow, between the two sides (in red). The red arrow with the two star-shaped markers delimitates the fastigium cerebelli.

Table 1

Clinical characteristics of the pathology group including perinatal outcome data.

Characteristic	Value
Age, years	31 (range: 21–45)
Gestational age, weeks	24.3±2.6 (range, 19–28)
Body mass index, kg/m ²	24.4±2.2
Gravidity	2.1±0.24
Parity	1.7±0.55
Karyotype analysis	5 abnormal ^a /22 analysed
Associated malformations	$n=15$ (50%) ^b
Intrauterine fetal deaths	$n=3$ (10%) ^c
Termination of pregnancy	$n=9$ (30%) ^d
Male: female ratio	1.5

Data are presented as mean ± SD where applicable.

^a Two cases of trisomy 18, two cases of trisomy 13, and one chromosome 4–6 translocation. Four of five karyotypic anomalies were in fetuses with the final diagnosis of DWM; the fifth case was associated with a patient with MCM.

^b Cardiac ($n=8$), brain ($n=7$), skeletal ($n=8$), renal ($n=3$), and gastrointestinal malformations ($n=2$).

^c One patient with DWM with no other malformations and a normal karyotype; one patient with VH and additional malformations; and one patient with confirmed DWM in trisomy.

^d Five patients with DWM, two with MCM, and two with VH both with additional malformations.

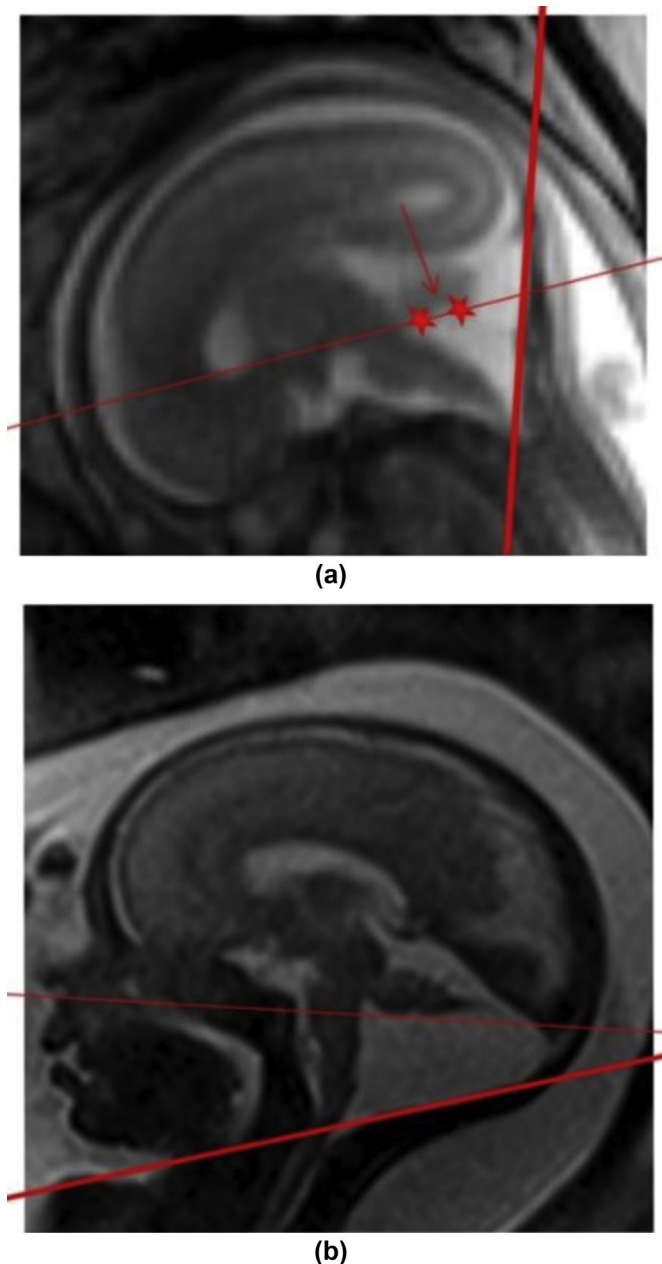


Figure 2 Measurement of VCA in fetuses with (a) BPC and (b) DWM. The VCA angles are 101° and 157°, respectively.

Table 2
Percentile distribution of vermian–crest angle (VCA) in relation to different subgroups.

Group (n)	5 th	10 th	50 th	90 th	95 th
Control (n=102)	48.79	50.52	64.49	78.29	84.96
Blake's pouch cyst (n=5)	93.76	94.26	100.25	106.16	107.47
Dandy–Walker malformation (n=12)	131.04	133.89	150.57	174.61	176.5

contrary, the VCA did not change in cases of VH (65.85 ± 5.35 ; $p=0.84$) nor in cases of MCM (64.34 ± 12.22 ; $p=0.95$). Box-and-whisker plots of the distribution of VCA in controls and pathological cases are shown in Fig 3.

Discussion

To the authors' knowledge, this is the first paper reporting the measurement of the VCA during prenatal MRI. Thanks to technological advancements, intrauterine MRI offers a detailed view of the anatomy of the prenatal PF, including both sides of the VCA in the midsagittal plane. The VCA is a technically easy-to-perform measurement and has the potentiality to improve the standardisation of MRI metrics in prenatal neuroimaging of the PF.

There are multiple reasons why the VCA should be assessed on prenatal MRI. First, MRI is an imaging method that is currently considered the reference standard for intrauterine diagnosis and is widely spreading in the field of prenatal medicine. A recent paper of Griffiths, published in *The Lancet* in 2016,³ reported that intrauterine MRI improved diagnostic accuracy and confidence for fetal brain abnormalities and led to management changes in a high proportion of cases. This finding, along with high patient acceptability, led the authors to propose that any fetus with a suspected brain abnormality on US should have intrauterine MRI to better inform counselling and management decisions.^{30,31} Secondly, the consistency of the VCA between intrauterine MRI and prenatal US may facilitate the communication between radiologists and maternal–fetal medicine (MFM) specialists, improving the diagnostic process and contributing, ultimately, to the optimal care of the patients.

Currently, to the authors' knowledge, only one intrauterine MRI study reporting on the measurement of the position of the vermian has been published.²⁷ In this present paper, the proposed measurements and distances between the vermian and the nearby structures are not always easy to trace. Indeed, to assess the PF, Vatansever *et al.*²⁷ proposed the measurement of a number of angles (i.e., the pontocerebellar gap width, the fourth ventricle angle, the primary fissure angle, the tegmento-vermian angle) that may be difficult to identify, because of the need for large magnification of the image, the special intrauterine MRI appearance of these structures with soft edges, and the requirement of a trained eye in order to avoid mistakes.

On the basis of the present results, measuring this angle on MRI appears feasible and reproducible. Indeed, the interobserver agreement is satisfactory, with a good ICC and a small 95% CI. The good reliability of the measurements may have useful implications for clinical practice. Looking forward to completed standardised MRI metrics in neuroimaging, the present measurements may be viewed as a reliable reference when investigating the anatomy of the prenatal PF, in particular at mid-trimester.

Interestingly, the VCA measurements on MRI are consistent with those performed on 3D US. This consistency strengthens the synergy between prenatal US and MRI. Indeed, rather than choosing between US or MRI, these two techniques are complementary and should be used to their maximum capability, arriving at a final diagnosis during a multidisciplinary discussion.²⁹

The fact that the VCA remained stable during the physiological development of the PF represented the basis for

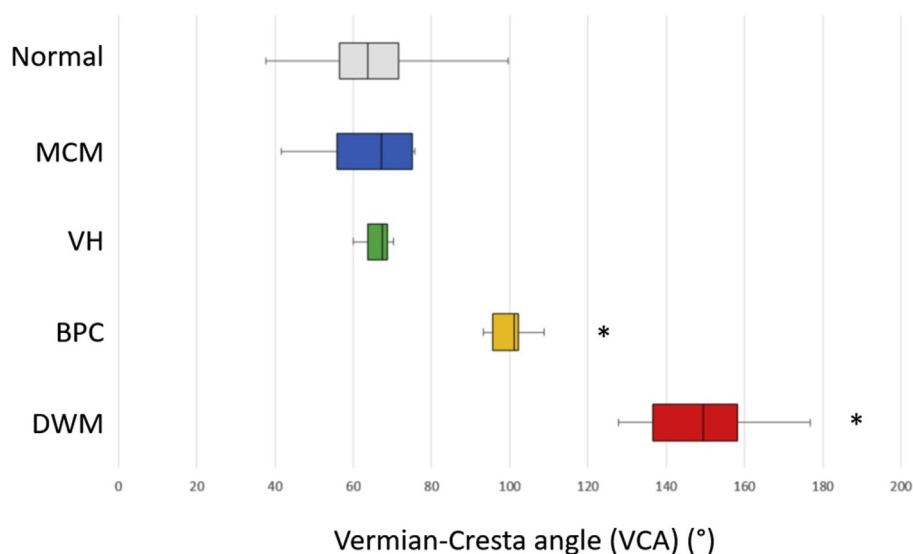


Figure 3 Box-and-whisker plot of the distribution of VCA (a) in controls and in fetuses with MCM, VH, BPC, and DWM. Medians are indicated by a line inside each box, 25th and 75th percentiles by box limits, and 5th and 95th percentiles by lower and upper bars, respectively. The VCA increased significantly (asterisk) in both BPC and DWM compared with controls.

the choice to compare the control group with those cases in which an abnormal PF was detected. Indeed, it was hypothesised that, in case of failure of normal embryological development of the vermis, which in turn leads to an abnormal size and rotation of the vermis, the proposed angle would have been affected and thus its measurement useful for objectively quantifying the degree and severity of an upward rotation.

The present results confirmed the a priori hypothesis, suggesting that measurement of the VCA has the potential to discriminate PF fluid collections associated with upward rotation of the cerebellum, including DWM, BPC, VH, and MCM. Distinguishing these entities prenatally is important, because of their different prognoses: a BPC is a risk factor for anatomical and chromosomal anomalies, but when isolated is probably a normal variant, whereas DWM and VH are true malformations frequently associated with other structural malformations, syndromes, and chromosomal or genetic diseases, as well as with cognitive, language, and behavioural dysfunction later in childhood.^{31,31} The differential diagnosis depends on visualisation of vermis size and position as well as the size and appearance of cisterna magna, the position of the tentorium and torcular, the relation between the fourth ventricle and cisterna magna, the presence of cisterna magna septa, and the choroid plexus position. All of these findings can be demonstrated *in utero* with sonography and/or MRI, but they are sometimes subjective findings and, even in expert hands, may be difficult to interpret, particularly early in gestation.

In the present series, the VCA seems to be helpful in providing additional information to discriminate this group of anomalies. The VCA was increased in the pathology groups compared with controls and in particular was significantly increased in cases of DWM and BPC, increasing with the severity of the condition. This finding is of value as the differential diagnosis of these two conditions is still

challenging in prenatal medicine. Interestingly, the VCA remained stable in cases of MCM and VH, independent of the severity of the condition in these cases. In these latter cases, however, the differential diagnosis can be performed easily on the basis of the size of the cisterna magna and of the vermis, respectively.

There were limitations of the study. The number of abnormal cases was relatively small, and they were investigated retrospectively. Further experience is certainly needed. Nevertheless, the spread of measurements between normal and abnormal cases and among the different categories of abnormalities suggests that the VCA may prove important in the differential diagnosis of fetal PF cystic anomalies, at least when used in combination with all the other existing criteria.⁶ Indeed, it is important to underline that the VCA alone does not diagnose all aspects of the malformations in the PF. As for VH, which is the fundamental part of DWM and strongly reflects the prognosis, the VCA could not reflect the degree of the vermis agenesis; however, the proper combination of the VCA with vermis biometry (all the diameters and volume), as well as the other parameters of the PF, may detect both the major and minor pathological conditions involved in the differential diagnosis of abnormal PF.

In light of these considerations, the VCA can be used as a possible categorisation of the major abnormalities of the PF, which should be properly validated in further multicentre studies with a major number of cases (Fig 4).

In conclusion, the present study shows how a new parameter of the PF, the VCA, can be obtained in a feasible and reproducible manner on intrauterine MRI with good agreement with prenatal 3D US, from 22 to 31 weeks of gestation.

The measurement developed in this study may enable accurate evaluation of the position of the cerebellar vermis in the PF as well as, in combination with other existing

<i>Vermis</i>					
<i>Findings</i>	Vermian-Crest Angle (VCA)	<i>Hypoplasia</i>	<i>Cisterna magna septa</i>	<i>Choroid plexus position</i>	<i>Diagnosis</i>
Enlarged Blake's pouch, enlarged posterior fossa, elevated torcula, (often hydrocephalus)	Increased	Yes: variable, may be severe	Invisible: apposed to side walls of cisterna magna	Inferior margin of Blake's pouch	Dandy-Walker malformation
Enlarged Blake's pouch, normal-sized posterior fossa, normal torcula	Normal	Yes: variable to intermediate	Invisible: apposed to side walls of cisterna magna	Inferior margin of Blake's pouch	Dandy-Walker variant or 'inferior vermian hypoplasia'
Enlarged Blake's pouch, normal-sized posterior fossa, normal torcula	Mild increased	No: may be misdiagnosed as 'inferior vermian hypoplasia'	Visible: bowed laterally	Superior margin of Blake's pouch	Blake's pouch cyst, a.k.a. persistent Blake's pouch
Enlarged Blake's pouch, enlarged posterior fossa	Normal	No	Visible: bowed laterally	Superior margin of Blake's pouch	Mega cisterna magna

Figure 4 A proposal of the categorisation of the major posterior fossa malformations including the VCA (modified from Robinson⁶).

parameters, help in the differential diagnosis of PF anomalies, providing the basis for proper management and counselling of these conditions.

Conflict of interest

The authors declare no conflict of interest.

References

- Rutherford MA. Magnetic resonance imaging of the fetal brain. *Curr Opin Obstet Gyn* 2009;**21**(2):180–6.
- Rutherford M, Jiang S, Allsop J, et al. MR imaging methods for assessing fetal brain development. *Dev Neurobiol* 2008;**68**(6):700–11.
- Griffiths PD, Bradburn M, Campbell MJ. Use of MRI in the diagnosis of fetal brain abnormalities in utero (MERIDIAN): a multicentre, prospective cohort study. *Lancet* 2017 Feb 4;**389**(10068):538–46.
- Limperopoulos C, Robertson LR, Estroff JA, et al. Diagnosis of inferior vermian hypoplasia by fetal MRI: potential pitfalls and neurodevelopmental outcome. *Am J Obstet Gynecol* 2006;**194**(4):1070–6.
- Barkovich AJ, Millen KJ, Dobyns WB. A developmental and genetic classification for midbrain–hindbrain malformations. *Brain* 2009;**132**:3199–230.
- Robinson AJ. Editorial. Inferior vermian hypoplasia — preconception, misconception. *Ultrasound Obstet Gynecol* 2014;**43**:123–36.
- Zalel Y, Gilboa Y, Gabis L, et al. Rotation of the vermian as a cause of enlarged cisterna magna on prenatal imaging. *Ultrasound Obstet Gynecol* 2006;**27**:490–3.
- Tilea B, Delezoide AL, Khung-Savatovski S, et al. Comparison between magnetic resonance imaging and fetopathology in the evaluation of fetal PF non-cystic abnormalities. *Ultrasound Obstet Gynecol* 2007;**29**:651–9.
- Katorza E, Bertucci E, Perlmann S, et al. Development of the fetal vermian: new biometry reference data and comparison of 3 diagnostic modalities—3D ultrasound, 2D ultrasound, and MR imaging. *AJNR Am J Neuroradiol* 2016;**37**:1359–66.
- Robinson AJ, Blaser S, Toi A, et al. The fetal cerebellar vermian: assessment for abnormal development by ultrasonography and magnetic resonance imaging. *Ultrasound Q* 2007;**23**:211–23.
- Spinelli M, Sica C, Di Meglio L, et al. Fetal cerebellar vermian circumference measured by 2-dimensional ultrasound scan: reference range, feasibility and reproducibility. *Ultrasound Int Open* 2016 Nov;**2**(4):E124–8.
- Clouchoux C, Guizard N, Evans AC, et al. Normative fetal brain growth by quantitative *in vivo* magnetic resonance imaging. *Am J Obstet Gynecol* 2012;**206**(2). 173. e1-178. 27.
- Hatab MR, Kamourieh SW, Twickler DM. MR volume of the fetal cerebellum in relation to growth. *J Magn Reson Imaging* 2008;**27**(4):840–5. 28.
- Scott JA, Habas PA, Kim K, et al. Growth trajectories of the human fetal brain tissues estimated from 3D reconstructed *in utero* MRI. *Int J Dev Neurosci* 2011;**29**(5):529–36.
- Ber R, Bar-Yosef O, Hoffmann C, et al. Normal fetal PF in MR imaging: new biometric data and possible clinical significance. *AJNR Am J Neuroradiol* 2015 Apr;**36**(4):795–802.
- Stazzone MM, Hubbard AM, Bilaniuk LT, et al. Ultrafast MR imaging of the normal PF in fetuses. *AJR Am J Roentgenol* 2000 Sep;**175**(3):835–9.
- Ghi T, Contro E, De Musso F, et al. Normal morphometry of fetal posterior fossa at midtrimester: brainstem–tentorium angle and brainstem–vermian angle. *Prenat Diagn* 2012 May;**32**(5):440–3.
- Illescas T, Martínez-Ten P, Bermejo C, et al. Brainstem–vermian and brainstem–tentorium angles: 3D ultrasound study of the intra- and inter-observer agreement. *J Matern Fetal Neonatal Med* 2017 Apr 5:1–5.
- Pinto J, Paladini D, Severino M, et al. Delayed rotation of the cerebellar vermian: a pitfall in early second-trimester fetal magnetic resonance imaging. *Ultrasound Obstet Gynecol* 2016 Jul;**48**(1):121–4.
- Meng X, Xie L. Quantitative evaluation of fetal brainstem–vermian and brainstem–tentorium angles by three-dimensional ultrasound. *Ultrasound Med Biol* 2014 Sep;**40**(9):2076–81.
- Contro E, Volpe P, De Musso F, et al. Open fourth ventricle prior to 20 weeks' gestation: a benign finding? *Ultrasound Obstet Gynecol* 2014 Feb;**43**(2):154–8.
- Zhao D, Liu W, Cai A, et al. Quantitative evaluation of the fetal cerebellar vermian using the median view on three-dimensional ultrasound. *Prenat Diagn* 2013 Feb;**33**(2):153–7.
- Spinelli M, Di Meglio L, Mosimann B, Di Naro E, Surbek D, Raio L. The Vermian-Crest Angle: A New Method to Assess Fetal Vermian Position within the Posterior Fossa Using 3-Dimensional Multiplanar Sonography. *Fetal Diagn Ther* 2018 Dec;**5**:1–8. <https://doi.org/10.1159/000494721>. PMID: 30517923.
- Volpe P, Contro E, De Musso F, et al. Brainstem–vermian and brainstem–tentorium angles allow accurate categorization of fetal upward rotation of cerebellar vermian. *Ultrasound Obstet Gynecol* 2012 Jun;**39**(6):632–5.
- Pilu G, Segata M, Ghi T, et al. Diagnosis of midline anomalies of the fetal brain with the three-dimensional median view. *Ultrasound Obstet Gynecol* 2006;**27**(5):522–9.

26. Terry KKoo, Li Mae Y. A Guideline of selecting and reporting intraclass correlation coefficients for reliability research. *J Chiropr Med* 2016 Jun;**15**(2):155–63.
27. Vatansever V, Kyriakopoulou V, Allsop JM, et al. Multidimensional analysis of fetal PF in health and disease. *Cerebellum* 2013;**12**:632–44.
29. Lei T, Xie HN, Zhu YX, et al. Date-independent parameters: an innovative method to assess fetal cerebellar vermis. *Cerebellum* 2015;**14**(3):231–9.
30. Kapur RP, Mahony BS, Finch L, et al. Normal and abnormal anatomy of the cerebellar vermis in midgestational human fetuses. *Birth Defects Res A Clin Mol Teratol* 2009;**85**:700–9.
31. Dekain LH, Kanel H, El-Bashir HO. Joubert syndrome labeled as hypotonic cerebral palsy. *Neurosciences (Riyadh)* 2014;**19**:233–5.